Effects of Transverse Magnetic Anisotropy on Current-Induced Spin Switching

Maciej Misiorny[1,2,3,*] and Józef Barnaś[3,4]

[1]Peter Grünberg Institut PGI-2, Forschungszentrum Jülich, 52425 Jülich, Germany
[2]JARA-Fundamentals of Future Information Technology, 52425 Jülich, Germany
[3]Faculty of Physics, Adam Mickiewicz University, Umultowska 85, 61-614 Poznań, Poland
[4]Institute of Molecular Physics, Polish Academy of Sciences, Smoluchowskiego 17, 60-179 Poznań, Poland

(Received 14 November 2012; published 23 July 2013)

Spin-polarized transport through bistable magnetic adatoms or single-molecule magnets (SMMs), which exhibit both uniaxial and transverse magnetic anisotropy, is considered theoretically. The main focus is on the impact of transverse anisotropy on transport characteristics and the adatom's or SMM's spin. In particular, we analyze the role of quantum tunneling of magnetization (QTM) in the mechanism of the current-induced spin switching, and show that the QTM phenomenon becomes revealed as resonant peaks in the average values of the molecule's spin and in the charge current. These features appear at some resonant fields and are observable when at least one of the electrodes is ferromagnetic.

DOI: 10.1103/PhysRevLett.111.046603 PACS numbers: 72.25.−b, 75.50.Xx, 85.75.−d

Experiments on electronic transport through individual atoms or molecules are at the forefront of the search for novel nanoelectronics and information processing technologies [1,2]. In this context, very prospective are magnetic atoms [3–5] and single-molecule magnets (SMMs) [6–10] with a large spin $S > 1/2$. If properly deposited onto a substrate, these quantum systems can acquire (in the case of atoms) [11] or retain (in the case of SMMs) [1,12] their intrinsic magnetic anisotropy—a property responsible for magnetic bistability. Especially attractive is the idea of incorporating magnetic adatoms or SMMs into spintronic devices [13], with the objective to use spin-polarized currents for manipulation of their magnetic moments [14,15]. Actually, the feasibility of this concept has already been experimentally proven for Mn and Fe adatoms [5]. One of the key conditions for successful applications is a sufficiently large uniaxial magnetic anisotropy constant D. Therefore, some efforts have been undertaken in order to synthesize new molecules with large D or to find other ways of anisotropy enhancement. It has been also demonstrated that magnetic anisotropy of an adatom or SMM can be systematically tuned, albeit in a limited range, e.g., by the environment adjustment [16], an external electric field [8], or mechanical stretching of a molecule [9].

Apart from the *uniaxial* magnetic anisotropy underlying the magnetic bistability, adatoms and SMMs usually possess also the *transverse* component of the anisotropy [6]. If the latter component is sufficiently large, it may lead to additional quantum effects, like oscillations due to the geometric Berry phase [17] or quantum tunneling of magnetization (QTM) [18,19]. Although the role of QTM in electronic transport has been studied extensively for normal electrodes [20–22], much less is known as to how it affects the spin-polarized transport [23,24]. Since QTM allows for the underbarrier transitions between the states on the opposite sides of the energy barrier, it may serve as an additional dephasing mechanism, and thus impede the control of the spin state by spin-polarized currents.

In this Letter we address the mechanism of current-induced spin switching in the presence of transverse anisotropy. We show that the conductance reveals peaks at voltages where the rate of direct (underbarrier) thermal transitions between degenerate states of lowest energy is equal to the rate of transition to the first excited state. Moreover, the transverse anisotropy significantly modifies the current-induced spin switching at some resonant fields, where the QTM phenomenon leads to resonant peaks in the field dependence of the average value of spin and charge current. These resonances are well pronounced in the field dependence of the derivative of current with respect to the magnetic field, and appear only when at least one electrode is ferromagnetic. We also show that the conductance generally depends on the relative orientation of the magnetic moments of the electrode and adatom or SMM. This effect follows from the interference of direct and indirect spin-conserving tunneling processes. In addition, a significant bias reversal asymmetry appears then in the transport characteristics.

Model.—Key features of magnetic adatoms and SMMs are captured by the giant-spin Hamiltonian [6],

$$\mathcal{H}_S = -DS_z^2 + \frac{E}{2}(S_+^2 + S_-^2) + \mathbf{S}\cdot\mathbf{B}, \qquad (1)$$

where the first and second terms stand for the *uniaxial* and *transverse* magnetic anisotropy, respectively, while the last term represents the Zeeman interaction, with $\mathbf{B} = (B_x, B_y, B_z)$ denoting an external magnetic field measured in energy units. Since we are interested here in systems with an energy barrier for spin switching, we assume $D > 0$. Without losing generality, we also assume positive perpendicular anisotropy constant, $E > 0$, and $0 \leqslant E/D \leqslant 1/3$ [6]. When $E \neq 0$, each of the $2S + 1$ eigenstates $|\chi\rangle$ of

the Hamiltonian (1), $\mathcal{H}_S|\chi\rangle = E_\chi|\chi\rangle$, is a linear combination of the eigenstates $|m\rangle$ of the S_z component. We label the states $|\chi\rangle$ with a subscript m, $|\chi\rangle \to |\chi_m\rangle$, which [as well as the numbers in Fig. 1(c)] corresponds to the S_z component of highest weight in the state $|\chi_m\rangle$, i.e., $|\chi_m\rangle \equiv |m\rangle$ for $E \to 0$. When $\mathbf{B} = (0, 0, B_z)$, the eigenstates $|\chi_m\rangle$ for $m = -S, \ldots, S$ can be written as $|\chi_m\rangle = \sum_k \langle m + 2k|\chi_m\rangle |m + 2k\rangle$, with integer k obeying the condition $-S \leqslant m + 2k \leqslant S$, and $\langle m|\chi_m\rangle$ being the amplitude of the state $|m\rangle$ in the eigenstate $|\chi_m\rangle$. Thus, the transverse anisotropy leads to mixing of the states $|m\rangle$, and therefore enables the QTM [19]. In the following, the index m shall be used only when necessary to avoid any confusion.

We consider an experimental configuration including tip of the scanning tunneling microscope (STM), and a substrate [which plays the role of second electrode] at which the adatom or SMM is deposited; see Fig. 1(a). Both the STM tip and substrate are characterized by noninteracting itinerant electrons, $\mathcal{H}_{\rm el} = \sum_{q\mathbf{k}\sigma} \varepsilon^q_{\mathbf{k}\sigma} a^{q\dagger}_{\mathbf{k}\sigma} a^q_{\mathbf{k}\sigma}$ ($q = t$ for the STM tip, and $q = s$ for the substrate), with the energy dispersion $\varepsilon^q_{\mathbf{k}\sigma}$, and $a^{q\dagger}_{\mathbf{k}\sigma}$ ($a^q_{\mathbf{k}\sigma}$) being the relevant creation (annihilation) operators ($\mathbf{k}$ is a wave vector, and σ is the electron spin index). In general, both electrodes can be magnetic, with spin-dependent density of states (DOS) ρ^q_σ at the Fermi level. By introducing the *spin polarization coefficient*, $P_q = (\rho^q_\uparrow - \rho^q_\downarrow)/(\rho^q_\uparrow + \rho^q_\downarrow)$, the DOS can be parametrized as $\rho^q_{\uparrow(\downarrow)} = (\rho^q/2)(1 \pm P_q)$ with $\rho^q = \rho^q_\uparrow + \rho^q_\downarrow$.

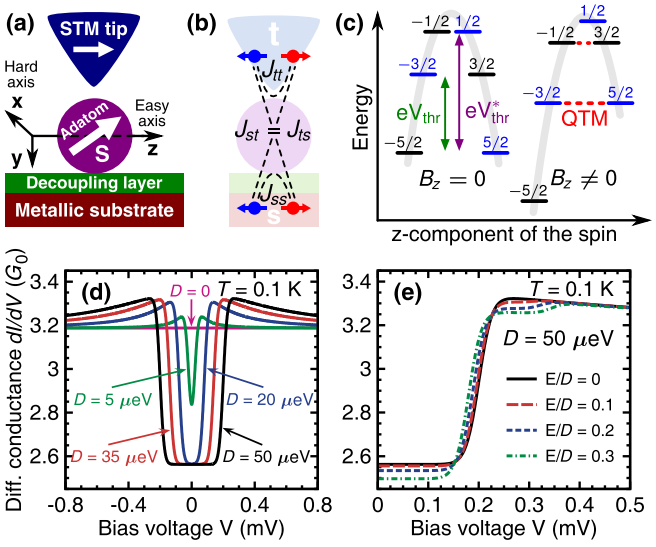

FIG. 1 (color online). (a) Schematic depiction of the system under consideration. (b) Examples of inelastic electron tunneling processes due to scattering of electron spin on the adatom's or SMM's spin. (c) Energy spectrum of the adatom or SMM for $S = 5/2$ in the absence (left) and presence (right) of an external magnetic field along the easy axis, $\mathbf{B} = (0, 0, B_z)$. Bottom panel shows the differential conductance as a function of bias voltage in the case of *nonmagnetic* electrodes ($P_t = P_s = 0$) for: (d) selected values of the uniaxial magnetic anisotropy constants D and absence of transverse anisotropy, $E = 0$; (e) several values of E for a given D. Remaining parameters: $T_d = 0.1$ eV, $\rho^t = \rho^s = 0.5$ eV^{-1} [thus $G_0 \approx 0.025\ 2e^2/h$], $\alpha = 1$ and $2\eta_t = \eta_s = 1$.

Electron tunneling processes in the STM geometry are modeled by the Appelbaum Hamiltonian [14,20,25,26],

$$\mathcal{H}_{\rm T} = \sum_{q\mathbf{k}\mathbf{k}'\alpha} \{T_d a^{q\dagger}_{\mathbf{k}\alpha} a^{\bar{q}}_{\mathbf{k}'\alpha} + \sum_{q'\beta} J_{qq'} \boldsymbol{\sigma}_{\alpha\beta} \cdot \mathbf{S} a^{q\dagger}_{\mathbf{k}\alpha} a^{q'}_{\mathbf{k}'\beta}\}, \quad (2)$$

with $\bar{q}$ to be understood as $\bar{s} \equiv t$ and $\bar{t} \equiv s$. Electrons can tunnel either directly between the two electrodes [the first term in Eq. (2)], or during the tunneling event they can interact with the adatom or SMM *via* exchange coupling [the second term in Eq. (2)]. The former processes are described by the tunneling parameter T_d, whereas the latter ones by the exchange parameter $J_{qq'}$; see Fig. 1(b). Both T_d and $J_{qq'}$ are assumed to be real, isotropic, and independent of energy and the electrodes' spin polarization. In the following discussion, we write $J_{qq'} = J\eta_q\eta_{q'}$, with η_q denoting the dimensionless scaling factor of the coupling between the adatom or SMM and the qth electrode (we fix $\eta_s = 1$). We also relate the parameters J and T_d as $J \equiv \alpha T_d$. Thus, T_d will serve as the key, experimentally relevant parameter [26], and α describes relation between the direct tunneling processes and those involving spin scattering of conduction electrons. For simplicity, electrodes' magnetic moments are assumed to be collinear with the easy axis of the adatom or SMM.

Method.—In the weak coupling regime, transport characteristics can be derived using the approach based on a master equation. The charge current flowing from the STM tip to the substrate is then given by $I = -e\sum_{\chi\chi'} \mathcal{P}_\chi \{\gamma^{ts}_{\chi\chi'} - \gamma^{st}_{\chi\chi'}\}$, where $-e$ is the electron charge, $\mathcal{P}_\chi$ is the probability of finding the SMM or adatom in the spin state $|\chi\rangle$ ($\equiv |\chi_m\rangle$), and $\gamma^{qq'}_{\chi\chi'}$ stands for the transition rate between the states $|\chi\rangle$ and $|\chi'\rangle$ ($\equiv |\chi_{m'}\rangle$) associated with electron tunneling between the electrodes q and q'.

For the sake of analytical clarity, we decompose the total current into two parts, $I = I_{\rm el} + I_{\rm in}$, where $I_{\rm el}$ represents the contribution due to *elastic* electron tunneling processes [the spin state $|\chi\rangle$ remains unchanged] and $I_{\rm in}$ is the *inelastic* term [with transitions between different states $|\chi\rangle$ and $|\chi'\rangle$]. In the second order approximation with respect to the electrode-SMM or adatom coupling, these two current components take the form

$$\frac{I_{\rm el}}{G_0} = \{1 + P_t P_s + 2\tilde{\alpha}\langle S_z\rangle(P_t + P_s)\}V + \sum_\chi \mathcal{P}_\chi \mathcal{V}_{\chi\chi}, \quad (3)$$

$$\frac{I_{\rm in}}{G_0} = \sum_\chi \sum_{\chi'(\neq\chi)} \mathcal{P}_\chi \mathcal{V}_{\chi'\chi}, \quad (4)$$

where

$$\mathcal{V}_{\chi'\chi} = \frac{\tilde{\alpha}^2}{e}\Big\{\Big[|\mathbb{S}^z_{\chi'\chi}|^2 + \frac{1}{2}\sum_{\kappa=\pm}|\mathbb{S}^\kappa_{\chi'\chi}|^2\Big]Z_-(\Delta^{\chi\chi'}_{eV})] + P_tP_s\Big[|\mathbb{S}^z_{\chi'\chi}|^2 - \frac{1}{2}\sum_{\kappa=\pm}|\mathbb{S}^\kappa_{\chi'\chi}|^2\Big]Z_-(\Delta^{\chi\chi'}_{eV}) + \frac{1}{2}(P_t - P_s)\sum_{\kappa=\pm}\kappa|\mathbb{S}^\kappa_{\chi'\chi}|^2 Z_+(\Delta^{\chi\chi'}_{eV})\Big\}. \quad (5)$$

In the equations above, $G_0 \equiv (\pi e^2/\hbar)\rho^t\rho^s|T_d|^2$, $\tilde{\alpha} \equiv \alpha\eta_t\eta_s$ and $\mathbb{S}^\kappa_{\chi'\chi} \equiv \langle\chi'|S_\kappa|\chi\rangle$ for $\kappa = z, \pm$. Accordingly, $\langle S_z\rangle = \sum_\chi \mathcal{P}_\chi \mathbb{S}^z_{\chi\chi}$. In addition, $\Delta^{\chi\chi'}_{eV} \equiv E_\chi - E_{\chi'} + eV$, where $eV = \mu_s - \mu_t$ stands for the difference in electrochemical potentials of the substrate (μ_s) and tip (μ_t), while $Z_\pm(\Delta^{\chi\chi'}_{eV}) \equiv \zeta(\Delta^{\chi\chi'}_{eV}) \pm \zeta(\Delta^{\chi\chi'}_{-eV})$ with $\zeta(x) \equiv x/\{1 - \exp[-x/(k_BT)]\}$ and T denoting temperature.

In order to evaluate the current from Eqs. (3) and (4), we need the probabilities $\mathcal{P}_\chi$. These can be obtained from the set of stationary master equations, $\forall_\chi$: $\sum_{\chi'}\{\mathcal{P}_{\chi'}\gamma_{\chi'\chi} - \mathcal{P}_\chi\gamma_{\chi\chi'}\} = 0$, with the probability normalization condition, $\sum_\chi \mathcal{P}_\chi = 1$. Here, the golden rule transition rates $\gamma_{\chi\chi'} = \sum_{qq'}\gamma^{qq'}_{\chi\chi'}$ for $\chi \neq \chi'$ are given by

$$\gamma^{qq'}_{\chi\chi'} = \frac{2\pi}{\hbar}|T_d|^2(\alpha\eta_q\eta_{q'})^2\zeta(\Delta^{\chi\chi'}_{\mu_q - \mu_{q'}}) \times\Big[\sum_\sigma \rho^q_\sigma\rho^{q'}_\sigma|\mathbb{S}^z_{\chi'\chi}|^2 + \rho^q_\uparrow\rho^{q'}_\downarrow|\mathbb{S}^+_{\chi'\chi}|^2 + \rho^q_\downarrow\rho^{q'}_\uparrow|\mathbb{S}^-_{\chi'\chi}|^2\Big]. \quad (6)$$

Nonmagnetic electrodes.—Consider a model system of spin $S = 5/2$, connected to nonmagnetic tip and substrate, and characterized by typical parameters observed in experiments, see the caption of Fig. 1. For vanishingly small transverse magnetic anisotropy ($E = 0$) and $|\mathbf{B}| = 0$, the Hamiltonian (1) is diagonal in the basis of the eigenstates of S_z. As a result, Eqs. (3) and (4) simplify significantly [14]: $I^{E=0}_{\rm el}/G_0 = \{1 + \tilde{\alpha}^2\langle S^2_z\rangle\}V$ and $I^{E=0}_{\rm in}/G_0 = (\tilde{\alpha}^2/2e)\sum_m \mathcal{P}_m\sum_{\lambda=\pm1}[A_\lambda(m)]^2 Z_-(\Delta^{m,m+\lambda}_{eV})$ with $A_\lambda(m) = [S(S+1) - m(m+\lambda)]^{1/2}$. For $D > 0$ and low T, the system occupies then with equal probabilities each of the metastable ground states $|\pm S\rangle$. When bias voltage $|V|$ increases, initially only the elastic tunneling processes contribute to transport, i.e. $I^{E=0}_{\rm el} \neq 0$ and $I^{E=0}_{\rm in} \approx 0$. When $|eV|$ becomes of the order of the threshold value $eV_{\rm thr} = D(2S-1) = 4D$ (for $S = 5/2$), see Fig. 1(c), the inelastic processes become activated and $I^{E=0}_{\rm in} \neq 0$, which appears as a characteristic step in the differential conductance, Figs. 1(d) and 1(e). This feature is typical of the systems exhibiting *easy-axis* magnetic anisotropy [4,5].

For $E > 0$ and a half-integer spin S, the eigenstates $|\chi_m\rangle$ are twofold degenerate (Kramers's doublets) and form two uncoupled sets $\{|\chi_{\pm S\mp 2k}\rangle\}_{k=0,1,\ldots,S-1/2}$ [21], schematically distinguished by different colors in Fig. 1(c). Mixing of the states corresponding to different values of m is also revealed in the expressions for current, $I^{E\neq0}_{\rm el}/G_0 = \{1 + \tilde{\alpha}^2\sum_k \mathcal{P}_{\chi_k}|\sum_m|\langle m|\chi_k\rangle|^2 m|^2\}V$ and $I^{E\neq0}_{\rm in}/G_0 = (\tilde{\alpha}^2/e)\sum_k\sum_{l(\neq k)}\mathcal{P}_{\chi_k}\{|\sum_m\langle\chi_l|m\rangle\langle m|\chi_k\rangle m|^2 + (1/2)\sum_{\lambda=\pm1}|\sum_m\langle\chi_l|m+\lambda\rangle\langle m|\chi_k\rangle A_\lambda(m)|^2\}Z_-(\Delta^{\chi_k\chi_l}_{eV})$.

The transverse anisotropy manifests as several new features in transport characteristics. First, for $|V| \lesssim V_{\rm thr}$ it leads to reduction of $I_{\rm el}$ [cf. the second terms of $I^{E=0}_{\rm el}$ and $I^{E\neq0}_{\rm el}$ given above], which appears as a decreased value of dI/dV, Fig. 1(e). Second, the transverse anisotropy effectively gives rise to a small reduction of $V_{\rm thr}$. Actually, at equilibrium, $V \approx 0$, the spin can directly oscillate between the two ground states $|\chi_{\pm S}\rangle$ as $\gamma_{\chi_{-S}\chi_S} = \gamma_{\chi_S\chi_{-S}} \propto k_BT$ [27], which is in contrast to $\gamma_{-SS} = \gamma_{S-S} = 0$ for $E = 0$. Such "underbarrier" oscillations will dominate until they are surpassed by transitions to the first excited spin dublet, which occurs at $|V| \approx V_{\rm thr}(E)$. It's worth emphasizing that the effect stems entirely from thermal fluctuations, so that the Kramers's degeneracy is not affected. Finally, for a significantly large transverse magnetic anisotropy, the second step in the differential conductance appears at $eV^*_{\rm thr} \approx 4D(S-1) = 6D$ (for $S = 5/2$), when direct spin excitations to the second excited Kramers' doublet become possible, Fig. 1(c). We note, however, that these features are clearly distinguishable only if $E \gg k_BT$.

Current induced magnetic switching.—In order to control the adatom or SMM's spin state by a spin-polarized current, at least one of the electrodes has to be magnetic [14,15]. Here, we choose it to be the tip, $P_t \neq 0$ and $P_s = 0$. Consider first the case of $E = 0$. When $|eV| < k_BT$, the system's spin can still fluctuate indirectly between the states $|\pm S\rangle$ as a result of stepwise "overbarrier" transitions. However, due to imbalance of the spin-up and spin-down electron tunneling processes, the systems's spin becomes locked in one of the ground states $|\pm S\rangle$ [depending on the bias polarization] for $|eV| \gtrsim k_BT$, Fig. 2(d). In consequence, the conductance is determined in the GMR fashion by the relative orientation of the tip's magnetization and the adatom's or SMM's spin, $dI/dV \propto 2\tilde{\alpha}P_t\langle S_z\rangle$, Fig 2(c). This behavior stems from the interference of direct tunneling and spin-conserving part of tunneling associated with the exchange interaction between tunneling electrons and magnetic core of the adatom or SMM, and also leads to the asymmetry in conductance with respect to bias reversal; see Fig. 2(c). Inelastic transport processes activated at $|V| \approx V_{\rm thr}$ enhance conductance [see the curve for $E/D = 0$ in Fig. 2(c)], but slightly reduce the absolute value of the average spin S_z component [see the curve for $E/D = 0$ in Fig. 2(d)].

The situation changes qualitatively for $E \neq 0$. For low voltages, the spin oscillates between $|\chi_{\pm S}\rangle$, like in the nonmagnetic case. However, due to the spin dependence of tunneling processes $\gamma_{\chi_{-S}\chi_S} \neq \gamma_{\chi_S\chi_{-S}}$, the spin generally resides longer in one of the two ground states [27]. At some voltage, transition rate to the excited state surpasses the transition rate between the two ground states and the spin

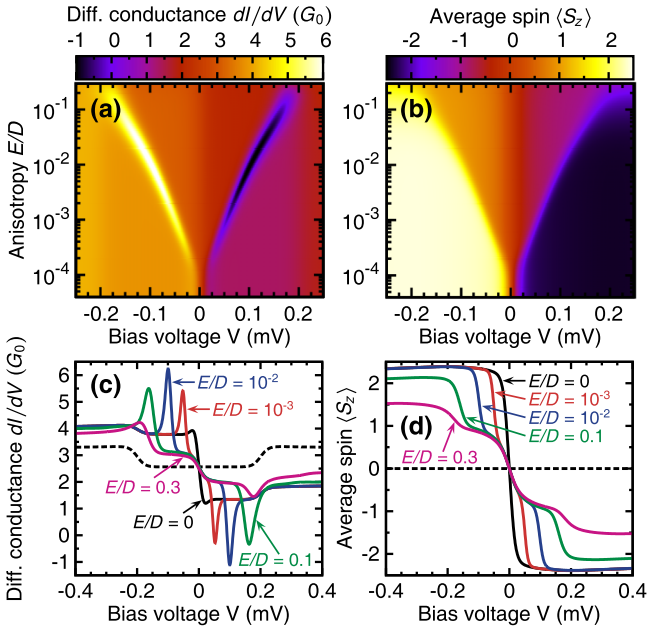

FIG. 2 (color online). Dependence of differential conductance (a) and the average value of the spin's zth component (b) on bias voltage and transverse magnetic anisotropy for $D = 50$ μeV and $P_t = 0.5$. Solid lines in (c) and (d) represent cross sections of (a) and (b), respectively, for selected values of E, while the dashed line corresponds to $E/D = 0$ and $P_t = 0$. Other parameters as in Fig. 1.

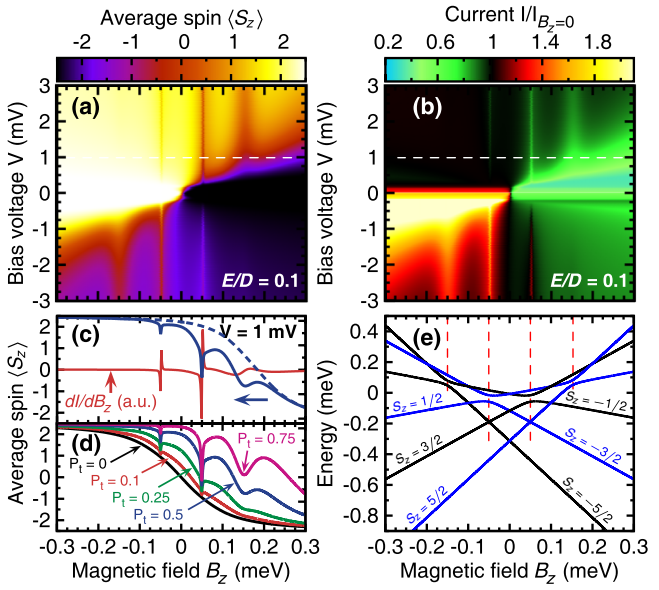

FIG. 3 (color online). (a) The average value of the spin's zth component and (b) the charge current shown as functions of an external magnetic field applied along the system's easy axis, B_z, and bias voltage for $D = 50$ μeV, $E/D = 0.1$ and $P_t = 0.5$. (c) Dark bold line represents a cross-section of (a) for indicated bias voltage [dashed line corresponds here to the case of $E = 0$], while bright bold line corresponds to dI/dB_z, shown here in arbitrary units. (d) Average spin for $V = 1$ mV, $E/D = 0.1$, and for several values of the tip polarization P_t. (e) Dependence of the system's energy spectrum on magnetic field B_z. Other parameters as in Fig. 1.

becomes locked in one of the two states $|\chi_{\pm S}\rangle$. This results in an additional peak in dI/dV, Fig. 2(c). Since the transition rate $\gamma_{\chi_{-S}\chi_S}$ increases with E, position of this peak moves towards larger voltage with augmenting E. Further rise in voltage leads to saturation of the conductance, and the saturated value only weakly depends on E. It's worth noting, however, that the strong mixing of spin states for large transverse anisotropy prevents the system's spin from aligning along the easy axis. Surprisingly, in the case of spin-polarized transport, the interplay of the underbarrier relaxation process introduced by the transverse magnetic anisotropy imposes the voltage barrier for switching the system's spin. Such a behavior doesn't take place in systems exhibiting purely uniaxial magnetic anisotropy.

When an external magnetic field is applied, one can achieve degeneracy of different states belonging to either of the two decoupled manifolds, see the right side of Fig. 1(c). This degeneracy, though, is not complete due to level repulsion, as shown in Fig. 3(e). Anyway, at the fields corresponding to the dashed lines in Fig. 3(e), quantum tunneling of magnetization takes place, which results in transitions between the two degenerate states. These transitions are clearly seen as resonant peaks in the average values of the molecules's spin, Figs. 3(a), 3(c), and 3(d), and current, Fig. 3(b). The resonant character of QTM is even more evident in the field dependence of dI/dB_z; see Fig. 3(c). Interestingly, the resonances due to QTM can be observed only when (at least) one of the electrodes is ferromagnetic, as follows from Fig. 3(d).

Conclusions.—In this Letter we have considered the influence of transverse magnetic anisotropy on spin polarized transport through magnetic adatoms or molecules, and in particular on the current-induced spin switching. First, we have demonstrated that mixing of states by transverse anisotropy leads to a decrease in conductance in the elastic transport regime (low voltage regime) and to appearing of the peaks at voltages where the system's spin becomes locked in one of the two ground states. When an external magnetic field is applied, the phenomenon of quantum tunneling of magnetization, which occurs at some resonant values of the magnetic field, results in resonant dips or peaks in the average value of the molecules's spin and in the charge current. It is worth emphasizing, however, that these effects can be observed only when the tip (and/or substrate) is ferromagnetic. Thus, spin-polarized transport spectroscopy may prove a useful experimental tool for studying the phenomenon of QTM.

It has been also shown that the conductance generally depends on the relative orientation of the average adatom's or SMM's spin and electrode's magnetic moment. This dependence stems from the interference of direct tunneling and spin-conserving tunneling connected with exchange

interaction between the electrons and adatom or SMM spin, and resembles the giant magnetoresistance effect in magnetic multilayers. It is also responsible for a significant asymmetry of transport characteristics with respect to the bias reversal and can be used to control spin switching of the adatom's or SMM's spin.

M. M. acknowledges support from the Foundation for Polish Science and the Alexander von Humboldt Foundation. The work has been supported by National Science Center in Poland as a research project in years 2010-2013 and the Project No. DEC-2012/04/A/ST3/00372.

*misiorny@amu.edu.pl

[1] M. Mannini *et al.*, Nat. Mater. **8**, 194 (2009).
[2] A. Khajetoorians, J. Wiebe, B. Chilian, and R. Wiesendanger, Science **332**, 1062 (2011); S. Loth, S. Baumann, C. Lutz, D. Eigler, and A. Heinrich, *ibid.* **335**, 196 (2012).
[3] A. J. Heinrich *et al.*, Science **306**, 466 (2004); F. Meier, L. Zhou, J. Wiebe, and R. Wiesendanger, *ibid.* **320**, 82 (2008); R. Wiesendanger, Rev. Mod. Phys. **81**, 1495 (2009).
[4] C. F. Hirjibehedin, C.-Y. Lin, A. F. Otte, M. Ternes, C. P. Lutz, B. A. Jones, and A. J. Heinrich, Science **317**, 1199 (2007); D. Serrate, P. Ferriani, Y. Yoshida, S.-W. Hla, M. Menzel, K. von Bergmann, S. Heinze, A. Kubetzka, and R. Wiesendanger, Nat. Nanotechnol. **5**, 350 (2010).
[5] S. Loth, K. von Bergmann, M. Ternes, A. F. Otte, C. P. Lutz, and A. J. Heinrich, Nat. Phys. **6**, 340 (2010); S. Loth, C. Lutz, and A. Heinrich, New J. Phys. **12**, 125021 (2010).
[6] D. Gatteschi, R. Sessoli, and J. Villain, *Molecular Nanomagnets* (Oxford University Press, New York, 2006).
[7] H. B. Heersche, Z. de Groot, J. Folk, H. van der Zant, C. Romeike, M. Wegewijs, L. Zobbi, D. Barreca, E. Tondello, and A. Cornia, Phys. Rev. Lett. **96**, 206801 (2006).
[8] A. S. Zyazin *et al.*, Nano Lett. **10**, 3307 (2010); E. Burzurí, A. S. Zyazin, A. Cornia, and H. S. J. van der Zant, Phys. Rev. Lett. **109**, 147203 (2012).
[9] J. J. Parks *et al.*, Science **328**, 1370 (2010).
[10] R. Vincent, S. Klyatskaya, M. Ruben, W. Wernsdorfer, and F. Balestro, Nature (London) **488**, 357 (2012).
[11] H. Brune and P. Gambardella, Surf. Sci. **603**, 1812 (2009).
[12] M. Mannini *et al.*, Adv. Mater. **21**, 167 (2009); S. Kahle *et al.*, Nano Lett. **12**, 518 (2012).
[13] L. Bogani and W. Wernsdorfer, Nat. Mater. **7**, 179 (2008).
[14] M. Misiorny and J. Barnaś, Phys. Rev. B **75**, 134425 (2007).
[15] C. Timm and F. Elste, Phys. Rev. B **73**, 235304 (2006); M. Misiorny, I. Weymann, and J. Barnaś, *ibid.* **79**, 224420 (2009); F. Delgado, J. J. Palacios, and J. Fernández-Rossier, Phys. Rev. Lett. **104**, 026601 (2010); F. Delgado and J. Fernández-Rossier, Phys. Rev. B **82**, 134414 (2010); J. Fransson, O. Eriksson, and A. V. Balatsky, *ibid.* **81**, 115454 (2010); B. Sothmann and J. König, *ibid.* **82**, 245319 (2010); N. Bode, L. Arrachea, G. S. Lozano, T. S. Nunner, and F. von Oppen, *ibid.* **85**, 115440 (2012).
[16] A. F. Otte, M. Ternes, K. von Bergmann, S. Loth, H. Brune, C. P. Lutz, C. F. Hirjibehedin, and A. J. Heinrich, Nat. Phys. **4**, 847 (2008).
[17] W. Wernsdorfer and R. Sessoli, Science **284**, 133 (1999); M. N. Leuenberger and E. R. Mucciolo, Phys. Rev. Lett. **97**, 126601 (2006).
[18] R. Sessoli, D. Gatteschi, A. Caneschi, and M. A. Novak, Nature (London) **365**, 141 (1993); L. Thomas, F. Lionti, R. Ballou, D. Gatteschi, R. Sessoli, and B. Barbara, *ibid.* **383**, 145 (1996); M. Mannini *et al.*, *ibid.* **468**, 417 (2010).
[19] D. Gatteschi and R. Sessoli, Angew. Chem., Int. Ed. **42**, 268 (2003).
[20] G.-H. Kim and T.-S. Kim, Phys. Rev. Lett. **92**, 137203 (2004).
[21] C. Romeike, M. R. Wegewijs, W. Hofstetter, and H. Schoeller, Phys. Rev. Lett. **96**, 196601 (2006); C. Romeike, M. R. Wegewijs, and H. Schoeller, *ibid.* **96**, 196805 (2006).
[22] G. Gonzalez and M. N. Leuenberger, Phys. Rev. Lett. **98**, 256804 (2007); G. González, M. N. Leuenberger, and E. R. Mucciolo, Phys. Rev. B **78**, 054445 (2008).
[23] R.-Q. Wang, R. Shen, S.-L. Zhu, B. Wang, and D. Y. Xing, Phys. Rev. B **85**, 165432 (2012).
[24] A. A. Khajetoorians *et al.*, Science **339**, 55 (2013).
[25] J. Appelbaum, Phys. Rev. **154**, 633 (1967); Phys. Rev. Lett. **17**, 91 (1966).
[26] Z. Nussinov, M. F. Crommie, and A. V. Balatsky, Phys. Rev. B **68**, 085402 (2003); J. Fransson, Nano Lett. **9**, 2414 (2009).
[27] See Supplemental Material at http://link.aps.org/supplemental/10.1103/PhysRevLett.111.046603 for details.